Screening of Magnetic Moments in PuAm Alloy: Local Density Approximation and Dynamical Mean Field Theory Study

J. H. Shim,[1] K. Haule,[1] S. Savrasov,[2] and G. Kotliar[1]
[1]Department of Physics, Rutgers University, Piscataway, New Jersey 08854, USA
[2]Department of Physics, University of California, Davis, California 95616, USA
(Received 25 May 2008; published 17 September 2008)

The puzzling absence of Pu magnetic moments in a PuAm environment is explored using the self-consistent dynamical mean field theory calculations in combination with the local density approximation. We argue that δ-Pu-Am alloys provide an ideal testbed for investigating the screening of moments from the single impurity limit to the dense limit. Several important effects can be studied: volume expansion, shift of the bare Pu on-site f energy level, and the reduction of the hybridization cloud resulting from the collective character of the Kondo effect in the Anderson lattice. These effects compensate each other and result in a coherence scale, which is independent of alloy composition, and is around 800 K.

DOI: 10.1103/PhysRevLett.101.126403 PACS numbers: 71.27.+a

The electronic structure of plutonium (Pu) is one of the outstanding issues in condensed matter theory. The volume of δ-Pu is between that of the early actinides, where the f electrons are itinerant, and the late actinides, where the f electrons are localized. Hence the view that the f electrons are very close to a localization-delocalization transition was put forward early on by Johansson [1]. This has been confirmed by numerous experiments [2–4] and theoretical developements [5–7], and motivated a study of the PuAm alloy, which is a unique system to investigate the effect of lattice expansion of δ-Pu (see Fig. 1). Since Pu is believed to be near a localization-delocalization transition, the theoretical expectation was that slight increase of the volume would result in an unscreened static magnetic moment. Surprisingly, an intensive program studying the Pu-Am mixtures, which has the effect of expanding the distance between the Pu atoms, has not shown an enhanced magnetic susceptibility, nor a narrowing of the peak at the Fermi level, as measured by photoemission experiment [8,9]. This seems naively at odds with both the quantum critical picture, and the dynamical mean field theory (DMFT) picture, and supports the suggestion, that the configuration of Pu in the solid is close to an inert $5f^6$ configuration [10], being essentially equivalent to Am configuration. Unfortunately, this picture cannot explain the results of high energy spectroscopies [4], nor the difference in specific heat between α-Pu and δ-Pu [5,11], nor the spectral properties [12]. Hence the puzzle of the absence of magnetic moments in Pu-Am alloys remains.

In this Letter, we provide a theoretical explanation of this puzzle using the LDA + DMFT method [13,14]. We find that indeed the moment remains well screened in agreement with experiment, and we identify the mechanism that compensates the effects of the lattice expansion. While the Pu-Am system cannot realize the unscreening of the local moment, and hence the approach to quantum criticality, it provides an ideal system in which to follow the transition from collective screening of moments, to single impurity spin screening of moments.

Within the LDA + DMFT method [13], the itinerant spd electrons are treated by the local density approximation (LDA) method [15], while for the electrons in the correlated f orbitals, all the local Feynman diagrams are summed up by solving an auxiliary quantum impurity problem, subject to a DMFT self-consistency condition

$$\frac{1}{\omega + \mu - E_{\mathrm{imp}} - \Sigma - \Delta} = \sum_{\mathbf{k}} [G_{\mathbf{k}}(\omega)]_{ff}. \qquad (1)$$

Here $\Delta(\omega)$ is the hybridization matrix of the auxiliary impurity problem, the matrix of impurity levels E_{imp} are computed by equating the high frequency expansion of the left and right side of Eq. (1), and $G_{\mathbf{k}}$ is the one electron Green's function $G_{\mathbf{k}} = 1/(O_{\mathbf{k}}(\omega + \mu) - H_{\mathbf{k}} - \Sigma)$. $H_{\mathbf{k}}$ and $O_{\mathbf{k}}$ are the LDA Hamiltonian and the overlap matrix in the projective orthogonalized LMTO basis set [16]. The quantum impurity solver is used to determine the local self-energy correction to the f-orbital Hamiltonian, which is a

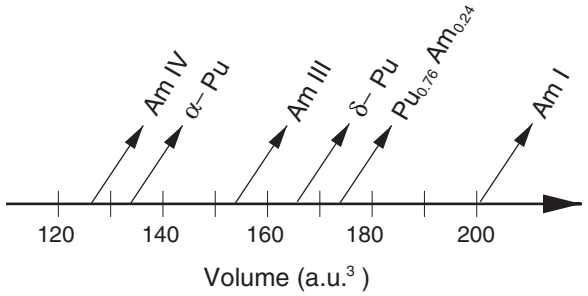

FIG. 1. The volume of Pu, Am and their alloys in various phases. The volume of Am-I at ambient pressure is 20% bigger than volume of δ-Pu. There is no structural phase transition between pure δ-Pu and $Pu_{0.25}Am_{0.75}$, and the structure remains fcc [26].

functional of the impurity levels, and the hybridization strength $\Sigma[E_{\rm imp}, \Delta]$. To solve the impurity problem, we used the vertex corrected one-crossing approximation method [17], and the results are further cross-checked by the continuous time quantum Monte Carlo method [18]. The Slater integrals F^k ($k = 2, 4, 6$) are computed by Cowan's atomic Hartree-Fock program including relativistic corrections [19] and rescaled to 80% of their atomic value, accounting for the screening in the solid. We use Coulomb interaction $U = 4.5$ eV, consistent with previous studies of Pu and Am [20,21].

Figures 2(a)–2(e) shows the calculated spectral function of $Pu_{1-x}Am_x$. Our LDA + DMFT results in Fig. 2 show a very favorable agreement with experiment. The spectral function of Pu atom, displayed in Fig. 2(f), is almost unchanged in PuAm alloys. The coherence scale, that determine the temperature below which the Pu moment is screened, remains roughly at 800 K in the alloys. The Am spectra is even more doping independent and shows no appreciate change when alloyed with Pu. This is not surprising since a very large pressure is needed to delocalize Am $5f$ electrons [21,22], and only the Am III and Am IV phase is known to be itinerant (see Fig. 1 for location of Am III and Am IV in volume diagram). Taking into account that the spectra of both Pu and Am are almost unchanged in alloys, the total DOS can be well approximated by a linear combination of the DOS of the two end compounds, as conjectured in Ref. [8].

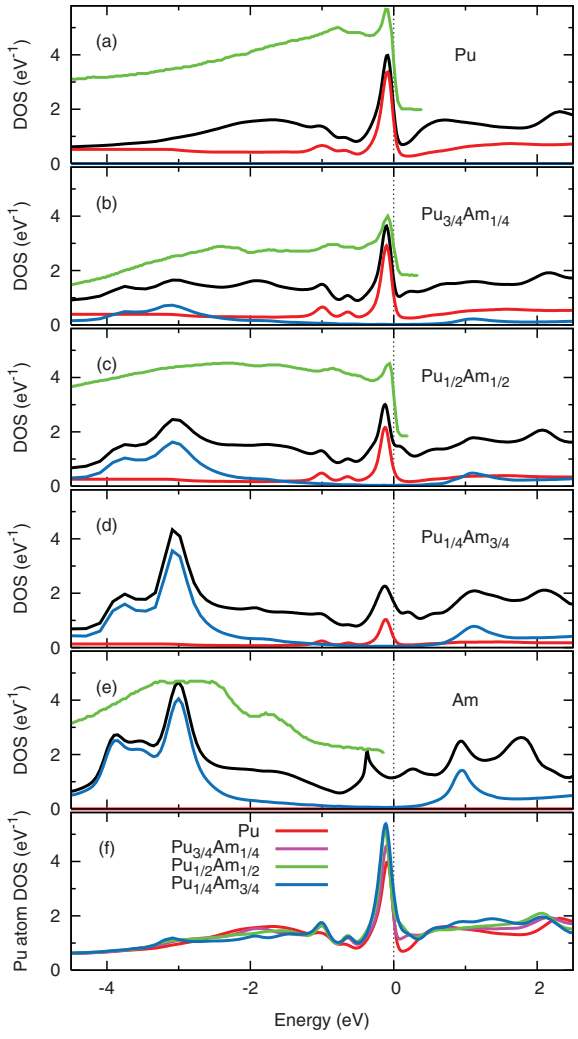

FIG. 2 (color). (a–e) The spectral function of $Pu_{1-x}Am_x$ in the fcc unit cell. To determine the lattice constant of the alloy, we used the linear interpolation between the two end compounds, δ-Pu and β-Am [8]. Total (black), Pu $5f$ (red), Am $5f$ (blue) spectrum are obtained by the LDA + DMFT method. The green lines show experimental photoemission spectrum at $x = 0.0$ (a), 0.20 (b), 0.36 (c), and 1.0 (e) (extracted from Ref. [8]). (f) The spectral function of Pu atom for various Am dopings.

In order to gain further insight into the puzzle of the doping independent coherence scale in the $Pu_{1-x}Am_x$ compound, we examine the important factors that govern the screening of the magnetic moments in our LDA + DMFT calculation. The coherence scale can be expressed analytically when the following two assumptions are made: (a) The atom has SU(N) symmetry and hence the spin-orbit, crystal field splittings, and Hund's coupling are absent, (b) the hybridization function Δ is frequency and temperature independent. In this case, the Kondo coherence scale can be estimated by $T_K \sim e^{-1/J}$, where J is

$$J \sim \frac{N}{\pi}\left(\frac{|\Delta''|}{E_{n+1} - E_n} + \frac{|\Delta''|}{E_n - E_{n-1}}\right) \qquad (2)$$

and E_n are the atomic energies corresponding to occupancy n, and N is degeneracy of the SU(N) model. In the extreme Kondo limit, the difference in the atomic energies are $E_{n+1} - E_n = U/2$ and $E_n - E_{n-1} = U/2$. The above assumptions are not realistic in Pu because of the strong multiplet effects and the strong frequency and temperature dependence of the hybridization function $\Delta(\omega, T)$. Nevertheless, the formula Eq. (2) gives the hint that the coherence scale is sensitive to the ratio $\langle|\Delta''|\rangle/\Delta E_f$, where $\langle|\Delta''|\rangle$ is average of the hybridization function in some low energy region, and ΔE_f is the difference between the ground state of the atomic f^6 configuration and the ground state of the atomic f^5 configuration. Namely, Pu $5f$ electrons are in mixed-valence state with an average occupancy close to $n_f \approx 5.2$ [5]; therefore, the dominant fluctuations are

$$e + 5f^5 \leftrightarrow 5f^6, \qquad (3)$$

where e is a conduction spd electron.

In turn, the $5f$ occupancy is correlated with the coherence scale, and the scale is smallest in the Kondo regime where n_f is integer [23]. In Fig. 3(a) we show the $5f$ occupancy for three different cases of chemical substitution and volume change. If the volume of the elemental Pu is changed without alloying, n_f is slightly decreasing with increasing volume [see red curve in Fig. 3(a)]. The magnitude of the n_f variation in the range of volumes, corresponding to α-Pu and Am is however surprisingly small,

only of the order of 0.06. If the volume is kept constant, but the the chemical composition is varied, the occupancy n_f is increasing with Am doping (green dots in Fig. 3(a) correspond to $x = 0$, $1/4$, $1/2$, and $3/4$ from left to right). The Pu atom is thus more mixed valent in the limit of small Pu concentration, i.e., single impurity limit. This might seem counterintuitive, but the increase in the coherence scale can be understood from the following consideration. The quasiparticle peak detected in $5f$ partial DOS creates a depletion in the conduction spd bands. This is traditionally called Kondo hole, which is always pinned at the Fermi level. The hybridization is thus decreased due appearance of quasiparticle peak, an effect termed by Noziere as "exhaustion." This Kondo hole does not form on Am atom, since there is no coherence peak on Am atom. Thus, if a single Pu atom in emerged in a lattice of Am atoms, the moment can be more efficiently screened by spd electrons, residing on neighboring Am sites. Finally, the blue dots in Fig. 3(a) show that the two effects largely cancel, when both the substitution and volume change are taken into account, and the $5f$ occupancy of $Pu_{1-x}Am_x$ is almost constant.

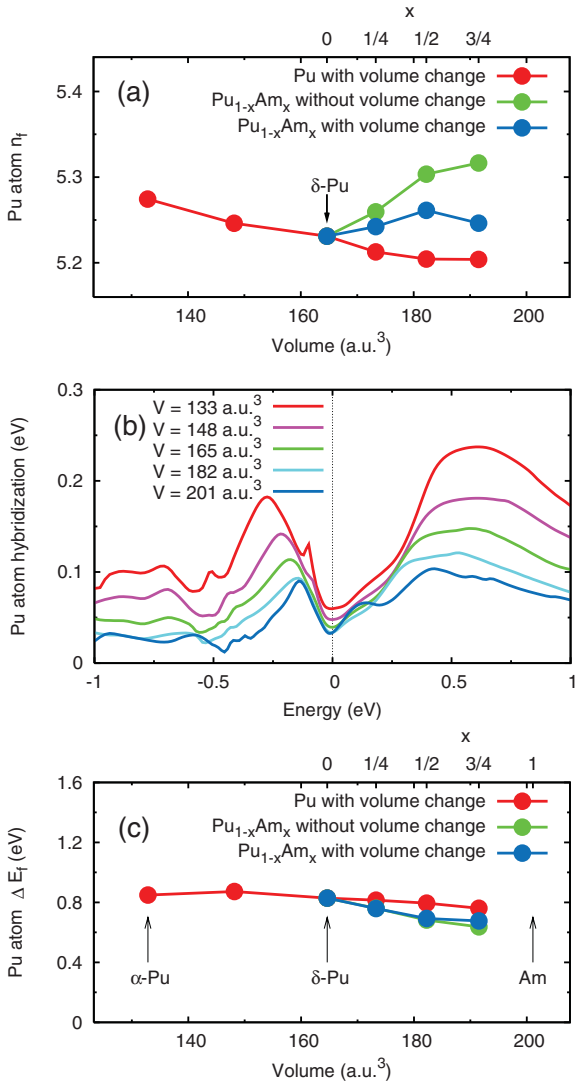

FIG. 3 (color). (a) The number of $5f$ electrons, n_f, as a function of volume (red dots), doping x at constant volume (green dots), and combination of both (blue dots). Note that $a = 8.1$, 8.7, and 9.3 a.u. correspond to the volume of α-Pu, δ-Pu and β-Am, respectively. (b) Volume dependence of hybridization function for Pu in the fcc phase. (c) The energy difference between the two most relevant atomic states, defined in the text.

The frequency dependent hybridization function $|\Delta''(\omega)|/\pi$ for elemental Pu at different volumes (no alloying), is shown in Fig. 3(b). The Kondo hole, i.e., depletion of hybridization at zero frequency, is clearly visible. Moreover, the hybridization changes substantially when volume is varied between the volume of α-Pu and Am volume. The change is between 30% at low energy and up to 50% at intermediate energies. This is a substantial change, which indeed unscreens magnetic moments and changes Pauli susceptibility into Curie-Weiss susceptibility, as shown in Ref. [6].

The Eq. (2) reveals that the coherence scale depends sensitively on the ratio $|\Delta''|/\Delta E_f$ rather than on the hybridization itself. In Fig. 3(c) we plot the smallest energy difference $\Delta E_f = E_6 - E_5$, which is the dominant contribution to the exchange coupling in Eq. (2). Here E_6 and E_5 are the ground state energies of the atomic f^6 and atomic f^5 configuration, respectively. In Figs. 3(c) we separate the effect of volume increase from the chemical substitution. It is clear from Fig. 3(c) that the energy difference is almost 3 times smaller than $U/2 \sim 2.25$ eV, the value that corresponds to the extreme Kondo limit [23]. The $5f^6$ atomic configuration has thus substantial overlap with the ground state wave function of the solid, as shown by valence histogram in Ref. [5]. It is also apparent from Fig. 3(c) that the volume increase has only a small effect on this energy difference (red curve). When alloying with Am, the change of ΔE_f is larger (blue dots) and is of the order of 25%. Since ΔE_f is decreasing, it thus partially compensates the decrease of hybridization with pressure, shown in Fig. 3(b). However, the magnitude of ΔE_f variation is too small to compensate the dramatic change of hybridization.

Finally, Fig. 4(a) shows the hybridization function for each composition of $Pu_{1-x}Am_x$ alloy for the case of a fixed volume. Because the dominant contribution to hybridization function is not the f-f hybridization but the f-spd hybridization [16], the overall magnitude of the hybridization is not changed. However, it is apparent from Fig. 4(a) that the chemical substitution of Pu by Am eliminates the hybridization dip, and therefore the Pu moment is even more efficiently screened by the spd electrons from neighboring Am atoms than neighboring Pu atoms. This elimination of Kondo hole by the chemical substitution by Am thus compensates the decrease of hybridization due to volume change. The net change of ΔE_f and the change of hybridization $\langle|\Delta''|\rangle$ due to both volume decrease and alloying compensate and lead to a constant coherence scale across the phase diagram.

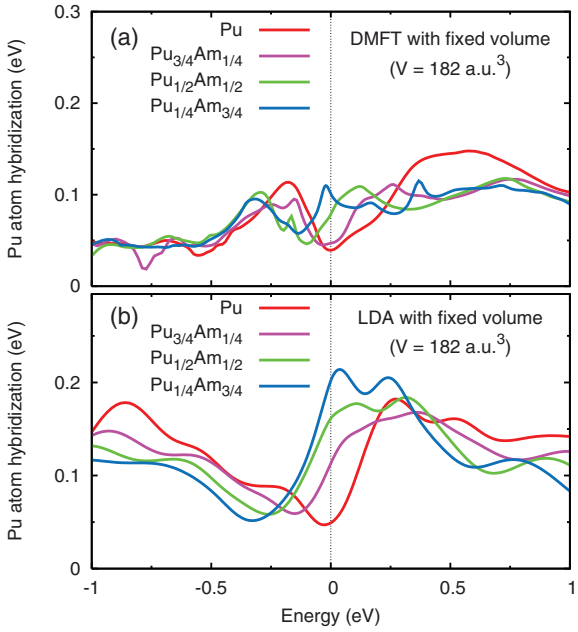

FIG. 4 (color). DMFT hybridization function for $Pu_{1-x}Am_x$ at fixed volume (a) computed within the self-consistent LDA + DMFT method, (b) within LDA by setting $\Sigma = 0$.

Figure 4(b) shows that the increase of hybridization due to alloying is present even on the LDA level, i.e., computing Δ by Eq. (1) and neglecting the self-energy corrections. However, the magnitude of the hybridization Δ and the magnitude of the change of Δ is substantially larger in LDA than in self-consistent LDA + DMFT method. The ''need for renormalization'' of the LDA hybridization was pointed out very early on [24,25] in the context of the description of cerium photoemission, when compared to a single impurity calculations.

To conclude, LDA + DMFT accounts for all the salient features of the experiments, and give new insights into the mechanism for spin compensation in the late actinides. It isolates two essential elements for the screening of the magnetic moment: hybridization and position of the f level. While hybridization is decreased by volume expansion, as naively expected, the substitution of Am eliminates the dip in the hybridization function, and at the same time shifts downward the position of f level. The three effects compensate each other, and the coherence scale remains around 800 K. Hence, the Pu-Am mixtures accentuates the mixed valent character of Pu.

Our work has important experimental consequences. While thermodynamic quantities such as susceptibility and specific heat should not exhibit significant modifications upon alloying, the same is not true for transport quantities. Optical conductivity is an excellent probe of the hybridization gap, and we predict that upon alloying, this hybridization gap will diminish while the dc resistivity will rapidly increases.

We acknowledge useful discussions with J. Allen, C. Marianetti. and M. J. Fluss. This work was funded by the NNSA SSAA program through DOE Research Grant DE-FG52-06NA26210.

[1] B. Johansson, Philos. Mag. **30**, 469 (1974).
[2] J. C. Lashley *et al.*, Phys. Rev. Lett. **91**, 205901 (2003).
[3] R. H. Heffner *et al.*, Phys. Rev. B **73**, 094453 (2006).
[4] K. T. Moore *et al.*, Phys. Rev. Lett. **90**, 196404 (2003); G. van der Laan *et al.*, Phys. Rev. Lett. **93**, 097401 (2004); K. T. Moore, G. van der Laan, M. A. Wall, A. J. Schwartz, and R. G. Haire, Phys. Rev. B **76**, 073105 (2007).
[5] J. H. Shim, K. Haule, and G. Kotliar, Nature (London) **446**, 513 (2007).
[6] C. A. Marianetti, K. Haule, G. Kotliar, and M. J. Fluss, Phys. Rev. Lett. **101**, 056403 (2008).
[7] G. Chapline, M. Fluss, and S. McCall, J. Alloys Compd. **444–445**, 142 (2007).
[8] N. Baclet *et al.*, Phys. Rev. B **75**, 035101 (2007).
[9] P. Javorsky, L. Havela, F. Wastin, E. Colineau, and D. Bouexiere, Phys. Rev. Lett. **96**, 156404 (2006).
[10] A. B. Shick, V. Drchal, and L. Havela, Europhys. Lett. **69**, 588 (2005); A. O. Shorikov, A. V. Lukoyanov, M. A. Korotin, and V. I. Anisimov, Phys. Rev. B **72**, 024458 (2005); L. V. Pourovskii *et al.*, Europhys. Lett. **74**, 479 (2006).
[11] L. V. Pourovskii, G. Kotliar, M. I. Katsnelson, and A. I. Lichtenstein, Phys. Rev. B **75**, 235107 (2007).
[12] J. X. Zhu *et al.*, Phys. Rev. B **76**, 245118 (2007).
[13] G. Kotliar *et al.*, Rev. Mod. Phys. **78**, 865 (2006).
[14] K. Held *et al.*, in *Quantum Simulations of Complex Many-Body Systems: From Theory to Algorithms*, edited by J. Grotendorst, D. Marks, and A. Muramatsu, NIC Series Vol. 10 (John von Neumann Institute for Computing, Julich, Germany, 2002), p. 175.
[15] S. Y. Savrasov, Phys. Rev. B **54**, 16470 (1996).
[16] A. Toropova, C. A. Marianetti, K. Haule, and G. Kotliar, Phys. Rev. B **76**, 155126 (2007).
[17] K. Haule, S. Kirchner, J. Kroha, and P. Wölfle, Phys. Rev. B **64**, 155111 (2001).
[18] K. Haule, Phys. Rev. B **75**, 155113 (2007).
[19] R. D. Cowan, *The Theory of Atomic Structure and Spectra* (Univ. California Press, Berkeley, 1981).
[20] S. Y. Savrasov, G. Kotliar, and E. Abrahams, Nature (London) **410**, 793 (2001).
[21] S. Y. Savrasov, K. Haule, and G. Kotliar, Phys. Rev. Lett. **96**, 036404 (2006).
[22] S. Heathman *et al.*, Phys. Rev. Lett. **85**, 2961 (2000).
[23] J. R. Schrieffer and P. A. Wloff, Phys. Rev. **149**, 491 (1966).
[24] J. W. Allen, J. Phys. Soc. Jpn. **74**, 34 (2005).
[25] O. Gunnarsson and K. Schönhammer, Phys. Rev. B **40**, 4160 (1989).
[26] F. H. Ellinger, K. A. Johnson, and V. O. Struebing, J. Nucl. Mater. **20**, 83 (1966).